Volumetric Behavior and Soil Water Characteristic Curve of Untreated and Lime-Stabilized Reactive Clay

Volumetric Behavior and Soil Water Characteristic Curve of Untreated and Lime-Stabilized Reactive Clay

Asmaa Al-Taie[1]; Mahdi Disfani, Ph.D.[2]; Robert Evans, Ph.D., CPEng[3]; Arul Arulrajah, Ph.D., CPEng[4]; and Suksun Horpibulsuk[5]

Abstract: This paper investigates the influence of lime stabilization of an expansive clay based on volumetric behavior and the soil–water characteristic curve (SWCC). The selected soil was a residual clay located in Victoria, Australia. Specimens treated with an optimum lime content (OLC) that was found to reduce swell potential were selected to investigate the SWCCs. Static compaction tests were conducted to establish the virgin compression surface. Hyprop (Meter Group, Pullman, Washington), filter paper, and the chilled mirror hygrometer were used to measure the SWCC at and below the surface at different net stress levels. To interpret the volumetric behavior of untreated and treated soil using the SWCC, swelling and collapse values were measured at various initial moisture contents and stress levels. The test results found that although the treated specimens were stabilized with lime at OLC, significant collapse and swelling potential were obtained when the lime-treated specimens were prepared at high suction value and wetted under low net stresses. **DOI: 10.1061/(ASCE)GM.1943-5622.0001336.** © *2018 American Society of Civil Engineers.*

Author keywords: Expansive clay; Lime stabilization; SWCC; Virgin compression surface.

Introduction

Expansive clays are common in many countries such as Australia, China, India, and the United States (Puppala et al. 2006). These clays have the ability to swell, shrink, and collapse due to wetting or drying (Haeri et al. 2016). Many studies have been conducted to obtain empirical correlations to predict swelling using Atterberg limits, liquidity index, and other properties that can be obtained by simple laboratory tests (Van Der Merwe 1964; Bryson et al. 2011; Richards et al. 1984). However, these studies did not interpret the behavior of swelling and collapse mainly because different soils with similar Atterberg limit values can exhibit very different volume change behavior patterns. Fredlund (2000) suggested that the swelling and collapse behavior of soils in an unsaturated condition can be better explained by considering the soil–water characteristic curve (SWCC).

The SWCC is a suction versus moisture content relationship at constant stress and temperature (Fredlund 2006; Fredlund and Vu 2003; Iyer et al. 2012; Jones et al. 2009; Krishnapillai and Ravichandran 2012). On the SWCC, the air entry value of the soil represents the suction value where air begins to enter the largest pores of the soil (Pasha et al. 2016). However, the residual water content is the water content where a large suction change is required to remove the additional water from the soil (Fredlund and Xing (1994). Thus, the SWCC is divided into three zones: (1) boundary effect zone, (2) transition zone, and (3) residual zone, as illustrated in Fig. 1 (Colmenares Montanez 2002; Fredlund 2006). Commonly, the air entry value, which is obtained at the end of the boundary effect zone and at the beginning of the transition zone, occurs close to the line of optimums (LOO) (Kodikara 2012).

Kodikara (2012) pointed out that most studies on the SWCC were conducted on stresses lower than the compaction stress (unloaded soil). Consequently, all outcomes achieved from laboratory tests have been restricted to being below the yield surface (Chinkulkijniwat et al. 2015; Colmenares Montanez 2002; Dineen et al. 1999; Romero Morales 1999). Kodikara (2012) described the volumetric behavior of a compacted unsaturated soil using a new framework based on net stress (σ), void ratio (e), and moisture ratio (e_w) (e_w = moisture content × specific gravity) as the main variables and suction as a dependent variable. The static compaction technique to generate virgin compression surface was also adopted by Kodikara (2012).

This paper adopted Kodikara's framework to study the influence of lime stabilization of an expansive clay soil based on volumetric behavior and the SWCC. The experimental program investigated the SWCC at the virgin compression surface to interpret the collapsible behavior, whereas the swelling behavior was investigated by studying the SWCC below the surface. In this study, the optimum lime content (OLC) (according to swelling potential) was selected for specimens prepared at optimum moisture content (OMC) and maximum dry density (MDD) to investigate the effect of the SWCC on stabilized soil behavior. The question raised here is whether a significant collapse and swelling potential can be obtained if a soil is stabilized with lime at the OLC and prepared at a higher suction (dry side of the OMC).

[1]Ph.D. Candidate, Swinburne Univ. of Technology, Melbourne, VIC 3122, Australia; Assistant Professor, Dept. of Civil Engineering, Univ. of Baghdad, Baghdad, Iraq. Email: aaltaie@swin.edu.au

[2]Senior Lecturer in Geotechnical Engineering, Dept. of Infrastructure Engineering, Melbourne School of Engineering, Univ. of Melbourne, Parkville, Melbourne, VIC 3010, Australia (corresponding author). Email: mahdi.miri@unimelb.edu.au

[3]Senior Lecturer, Dept. of Civil Engineering, Swinburne Univ. of Technology, Melbourne, VIC 3122, Australia. Email: robertevans@swin.edu.au

[4]Professor, Dept. of Civil Engineering, Swinburne Univ. of Technology, Melbourne, VIC 3122, Australia. Email: aarulrajah@swin.edu.au

[5]Professor, Dept. of Civil Engineering, Suranaree Univ. of Technology, Nakhon Ratchasima 30000, Thailand; Adjunct Professor, Swinburne Univ. of Technology, Melbourne, VIC 3122, Australia. Email: suksun@g.sut.ac.th

Note. This manuscript was submitted on September 14, 2017; approved on July 30, 2018; published online on November 28, 2018. Discussion period open until April 28, 2019; separate discussions must be submitted for individual papers. This paper is part of the ***International Journal of Geomechanics***, © ASCE, ISSN 1532-3641.

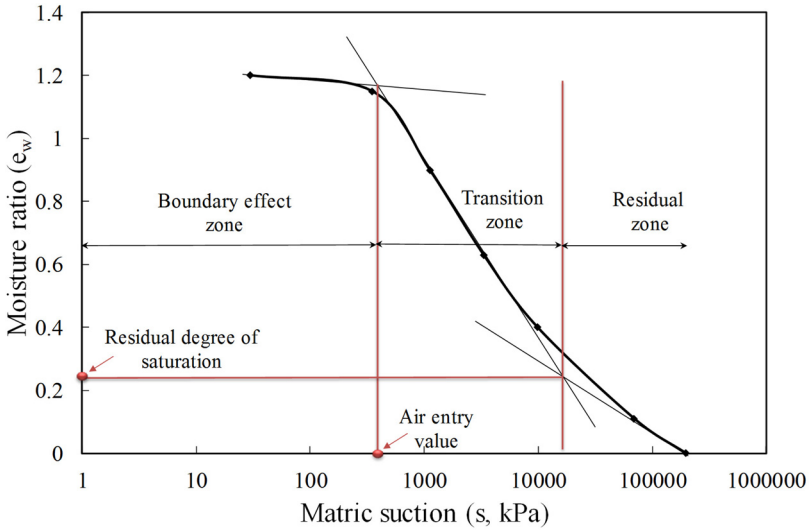

Fig. 1. General SWCC structure according to Colmenares Montanez (2002).

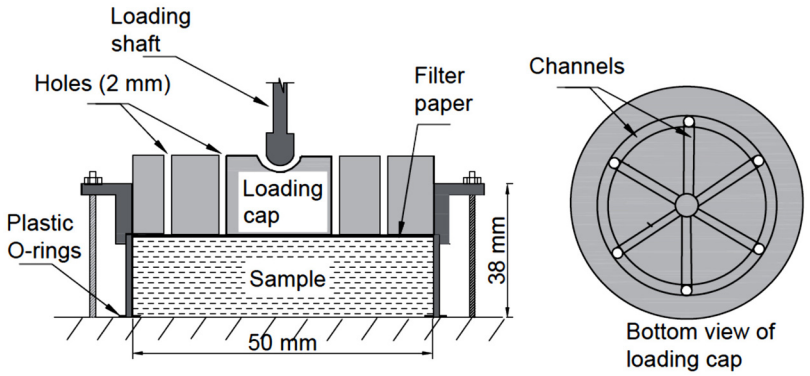

Fig. 2. Setup of static compaction and state path tests.

Material and Methodology

A series of laboratory tests were performed to interpret the influence of lime stabilization of an expansive clay soil based on volumetric behavior and the SWCC. Firstly, standard Proctor compaction and 1-D swell tests were conducted to obtain the OLC based on swelling potential. Secondly, static compaction tests were conducted to establish compaction curves at different net stresses, and subsequently, the virgin compression surface was generated. Thirdly, Hyprop (UMS 2013), filter paper, and a chilled mirror hygrometer [WP4C (Meter Group, Pullman, Washington)] were used to measure the SWCC at and below the virgin compression surface at different net stress levels. Fourthly, collapse and swelling potential were measured at various initial moisture contents and stress levels.

Material

The soil selected for this study was a residual clay weathered from a quaternary basalt deposit located in Victoria, Australia (McAndrew and Marsden 1973). This soil was collected at a depth of 1–2 m. The specific gravity was measured and found to be 2.71 (ASTM 2010). According to ASTM (2007), sand, silt, and clay contents were found to be 4, 43, and 53%, respectively. The liquid limit, plastic limit, plasticity index, and linear shrinkage were measured and found to be 73.7, 23.2, 50.5, and 20.3%, respectively (AS 2008; ASTM 2000a). Consequently, this soil was classified as clay with high plasticity (CH) (ASTM 2011).

Experiment Procedure for Determination of the OLC

The standard Proctor compaction test was performed according to ASTM (2000b) to measure OMC and MDD for the untreated clay specimens. To prepare the untreated sample, the clay was first dried at 105°C for 24 h and then mixed with different moisture contents and left for 7 days in sealed polythene bags for equilibrium. However, for the treated clay, the compaction procedure outlined by Ciancio et al. (2014) was considered. Dry sample was mixed with lime (at 2, 3, 4, 6, and 8% lime content). Water was then added and mixed, and the mixture was left for 1 h; then the whole compaction procedure was achieved within 45 min. The same procedure was followed for various moisture contents.

A series of 1-D swell tests were also performed on the untreated and treated samples. The swell test specimens were compacted to OMC and MDD. The treated samples were allowed to cure for 1, 7, and 28 days. During curing, the relative humidity was kept at 95% and the temperature at 20 ± 2°C. Once the specimens were placed in an oedometer device, all specimens were saturated under a pressure of 25 kPa to simulate field stress conditions.

Experiment Procedure for Generation of the Virgin Compression Surface

For untreated and treated specimens, the virgin compression surface was generated by compaction curves at various net stresses. Static compaction tests were conducted at different moisture ratios to develop each compaction curve. The specimens were compacted statically with a varying moisture content from 0 to 50%, while the static compaction varied from 2 kPa to 4,000 kPa. The stress of 2 kPa represented the loosest state and resulted from the weight of the loading cap.

A static compaction setup was designed, as presented in Fig. 2, to establish the virgin compression surface. For the untreated clay, the specimens were dried and then mixed with water at various moisture contents. The mixtures were sealed and left in plastic bags for soil–water homogeneity. To minimize friction between the specimen and the wall of the mold, silicon grease was used. The specimen was then set into the mold. The base of the mold should be blocked, and filter paper was placed between the top of the specimen and loading cap to catch any water leaving.

Table 1. OMC and MDD values of untreated and lime-treated samples

Lime (%)	OMC (%)	MDD (kN/m^3)
0	25	14.9
2	26	14.78
3	26.5	14.68
4	26.9	14.61
6	27.8	14.54
8	28.5	14.41

Table 2. Swelling values of untreated and lime-treated samples

	Swelling after curing (%)			
Lime (%)	0	1	7	28
0	6.3	—	—	—
2	—	3.3	2.7	2.5
3	—	2.4	1.87	1.68
4	—	0.4	0	0
6	—	0	0	0
8	—	0	0	0

For unsaturated specimens, the net normal stress is defined as the excess of total normal stress over the pore air pressure. The stress rate was controlled to guarantee that the air pressure was equal to atmospheric pressure. At the dry side of the LOO, air is free to drain easily, even under high rates of stress (fast loading). Thus, it can be assumed that excess air pressure will not build up during compression, and hence, the applied stress is equal to the net stress. A set of compression paths were plotted in e-e_w space under different stress rates to develop the loading wetting state boundary surface (LWSBS) contours at the dry side of the LOO. When the moisture content of specimens passed the LOO, slow stress rates were applied to establish the drained states, avoiding excess air pressure to build up. Therefore, it is assumed that the excess air pressure will not build up, and consequently, the applied stress will be equal to the net stress. Several drained constant net stress contours between the LOO and saturation line [normally consolidated line (NCL)] were developed to establish the LWSBS contours. To develop a drained constant net stress contour, specimens at different moisture contents were compressed. Once the moisture content reached the LOO, a much slower stress rate was applied. According to these developed constant net stress contours, the specimens at the dry side of the LOO were compacted at a high stress rate (i.e., 20 kPa/min for stresses $\leq$ 1,000 kPa and 100 kPa/min for stresses $>$ 1,000 kPa). Once the moisture content arrived at the LOO, the stress rate was decreased to 0.5 kPa/min for stresses $\leq$ 1,000 kPa and 1.5 kPa/min for stresses $>$ 1,000 kPa. During the test, the cell was covered with plastic wrap, and the load frame was placed in a plastic bag to reduce water content loss due to evaporation. At the end of the test, the final void ratio was calculated measuring required inputs such as mass, volume. and water content and using soil phase relationship. The previous steps were repeated for other specimens at various moisture contents and net stress levels to generate the surface.

The procedure to generate the surface for the lime-treated specimens was slightly different. To prepare a compacted treated specimen statically, water was added to the dry soil–hydrated lime mixture. At moisture contents higher than the LOO, the stress rate was

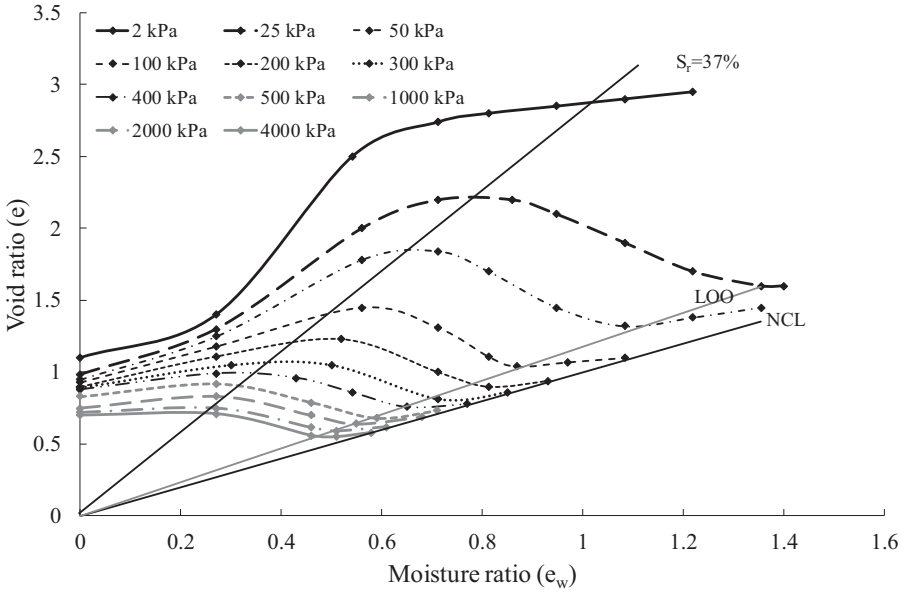

Fig. 3. Virgin compression surface for the expansive soil.

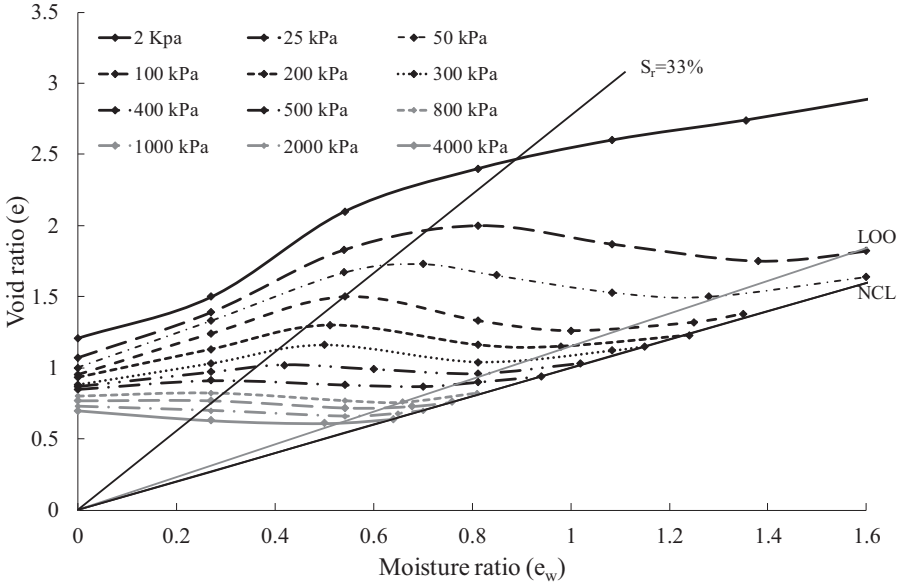

Fig. 4. Virgin compression surface for the treated expansive soil with 4% lime.

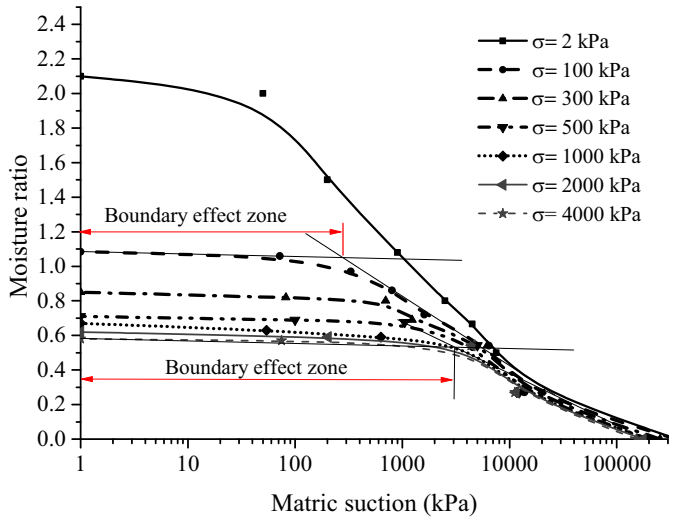

Fig. 5. SWCC at the virgin compression surface (untreated clay).

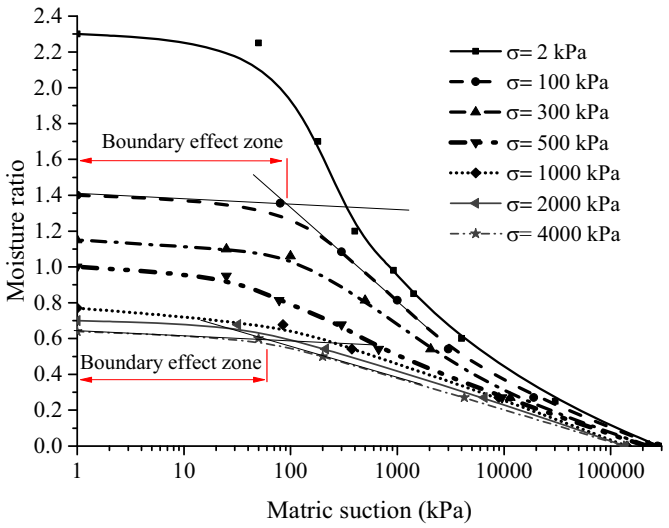

Fig. 6. SWCC at the virgin compression surface (lime-treated clay).

increased to 4 kPa/min for static stresses ≤ 1,000 and 8 kPa/min for static stresses > 1,000 kPa. The reason for raising the stress rate was due to the cation exchange and the flocculation process beginning as soon as the water was added.

Experiment Procedure for Generation of Suction Distribution at the Virgin Compression Surface

To identify the suction distribution of the untreated and lime treated clays at the surface in e-e_w space, it was important firstly to measure the SWCC at the surface under different net stresses. Specimens were prepared at various moisture ratios and then compacted statically at different net stress levels. The values of suction were then measured by using the Hyprop or filter paper or chilled mirror hygrometer (WP4C) device based on the respective moisture contents. The Hyprop, which contains tensiometers, measures the matric suction of a soil within a range of 0–1,500 kPa (Murray and Sivakumar 2010). However, the WP4C relies on the chilled mirror dewpoint technique, which measures the total suction (i.e., matric suction and osmotic suction) of the soil within a range of 1,500–60,000 kPa (ASTM 2016; Murray and Sivakumar 2010). As the filter paper technique can measure total and matric suctions, the osmotic suction was obtained at any moisture content (ASTM 1994). For example, to produce the SWCC for the untreated clay at a planned compaction stress, the given steps were followed:

1. Specimens at different moisture contents were prepared and compacted statically to the planned compaction stress. The void ratios were then calculated.
2. At high moisture contents (i.e., range of matric suction from 0 to 1,500 kPa). The Hyprop was used to measure the matric suction.
3. The WP4C was used to measure the total suction at low moisture contents.
4. The filter paper was used to measure the total and matric suction at different moisture contents, and subsequently, the osmotic suction for expansive clay was obtained.

5. Steps 1 to 4 were repeated for specimens compacted statically at different net stress levels.

The same procedure was followed for the lime-treated specimens except the specimens were cured for 7 days after compaction, and then the suction values were measured.

Secondly, the relationship between suction and void ratio was obtained at different net stresses. Consequently, the suction distribution of both clays were plotted.

Experiment Procedure for Generation of Suction Distribution below the Virgin Compression Surface

To obtain the SWCC below the surface, specimens were prepared under different moisture ratios, compressed statically to a certain net stress, and then unloaded to an operational stress. The specimens were then wetted with different amounts of water at that operational stress. The suction of each specimen (after wetting) was measured. Consequently, the SWCCs were obtained for each net stress level. For the treated specimens, the same procedure was followed except the specimens were cured for 7 days. The volume changes after wetting were recorded, and void ratio was measured when the change in the volume change became negligible. Consequently, the relationship between void ratio and matric suction was obtained. Finally, the suction distribution below surface was plotted.

It is important to note that after wetting the specimens to a certain amount of water at a certain operational stress and when the volume change became negligible, the specimens were removed from the setup, and the suction values were measured using the Hyprop or WP4C. This means that the suction values will be measured under zero operational stress. Therefore, it is important to measure the slope of the unloading–reloading curve (κ) for the untreated and lime-treated clays at different moisture contents.

Experiment Procedure for Measurement of the Slope of the Unloading–Reloading Curve

A series of tests were performed to investigate the behavior of unloading–reloading of an unsaturated expansive clay soil (untreated

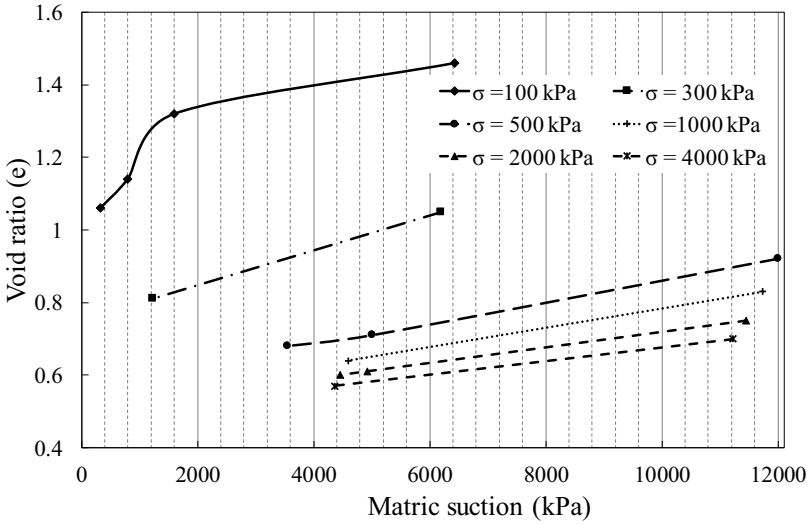

(a)

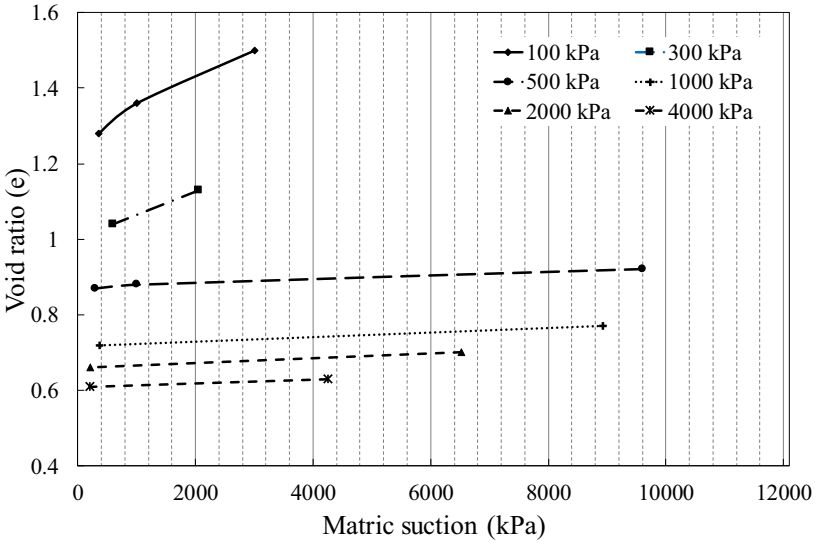

(b)

Fig. 7. Void ratio–suction relationship at equal total vertical stress (at the surface): (a) untreated clay; and (b) lime-treated clay.

and treated with lime) at moisture contents varying from 0 to 22%. Specimens were compacted to different stress levels and then unloaded to 25, 100, 300, 500, 1,000, 2,000, and 4,000 kPa.

Test Results

OLC

The OMC and MDD of untreated and treated (2, 3, 4, 6, and 8%) specimens are presented in Table 1. The swell results given in Table 2 reveal that a significant reduction in swell behavior occurred for the specimens treated with 2% lime and eliminated with the addition of 4% lime (Al-Taie et al. 2018). Hence, from the swell test results, the OLC for this clay was found to be 4%. This percentage was used in this study.

Virgin Compression Surface

Figs. 3 and 4 present the virgin compression surface for the untreated and 4% lime treated expansive clay, suggesting that the moisture ratio decreased as the void ratio increased. For very dry soils, the moisture ratio increased with an increasing void ratio. This behavior appears to be related to the weakening of the effect of suction in forming strong contact between particles. This can consequently lead to larger macro void space.

Slope of the Unloading–Reloading Curve

For the untreated clay, the average values of κ over this range of moisture contents ranged between 0.006 and 0.045. As the values of κ were very small, it could be considered as zero. For the treated clay specimens, the values of κ ranged between 0.016 and 0.028,

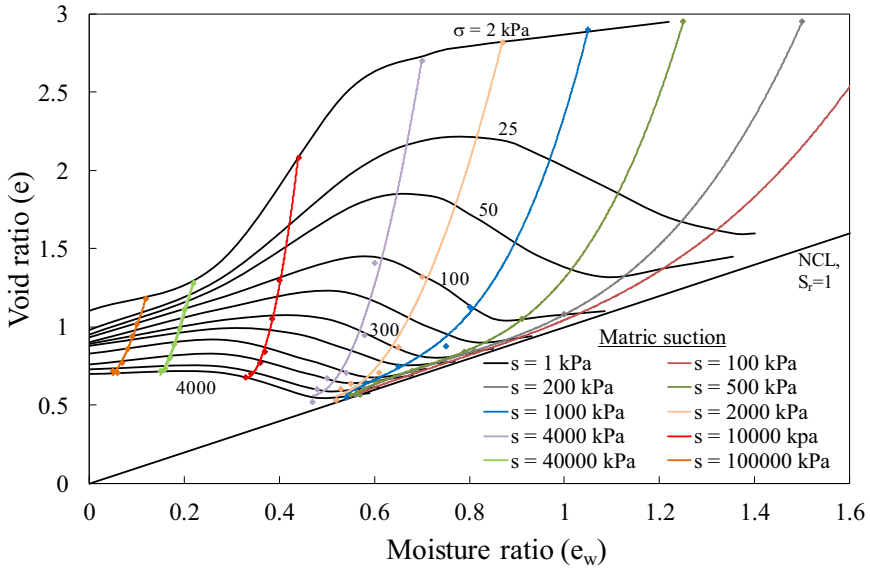

Fig. 8. Suction distribution at the virgin compression surface (untreated clay).

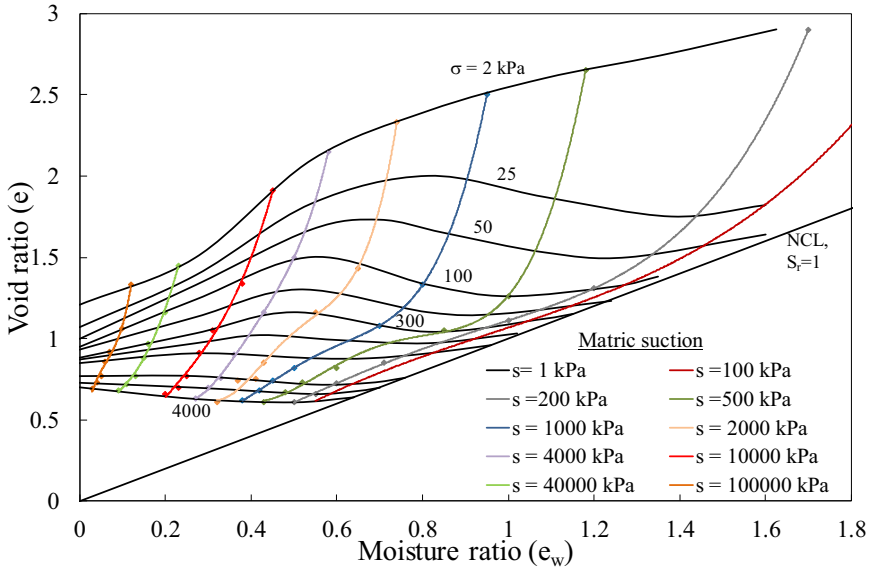

Fig. 9. Suction distribution at the virgin compression surface (lime-treated clay).

which can also be considered to be practically equal to zero. Hence, it can be assumed that the void ratio value after loading to a planned compaction stress is equivalent to the void ratio after unloading to a planned operational stress.

Interpretation of Volumetric Behavior of Unsaturated Clay Using the SWCC

Suction Distribution at the Virgin Compression Surface

Figs. 5 and 6 present the SWCC at the surface for the untreated and lime-treated clay samples. The osmotic suction for the untreated clay was measured and found to vary from 80 to 100 kPa. As the increase in cation concentration in the water leads to an increase in osmotic suction (Zhao et al. 2014), the osmotic suction for the lime treated clay varied from 340 to 380 kPa.

By measuring void ratio values after compaction, the relationship between void ratio and matric suction is presented in Fig. 7. The range of this relation started from a moisture ratio corresponding to the maximum void ratio. It was necessary to identify the moisture ratio range where the void ratio started from maximum to minimum value for a certain net stress level. Figs. 3 and 4 found that the maximum void ratio value approximately occurred at the degree of saturation (S_r) of 37 and 33% for the untreated and treated clay. Hence, for a certain net stress, the relationship between suction and void ratio was studied for the S_r range starting from 37 and 33% to the LOO, as presented in Fig. 7.

By identifying the moisture ratio, void ratio, net stress, and suction for each specimen, the suction distribution at the surface was plotted, as given in Figs. 8 and 9.

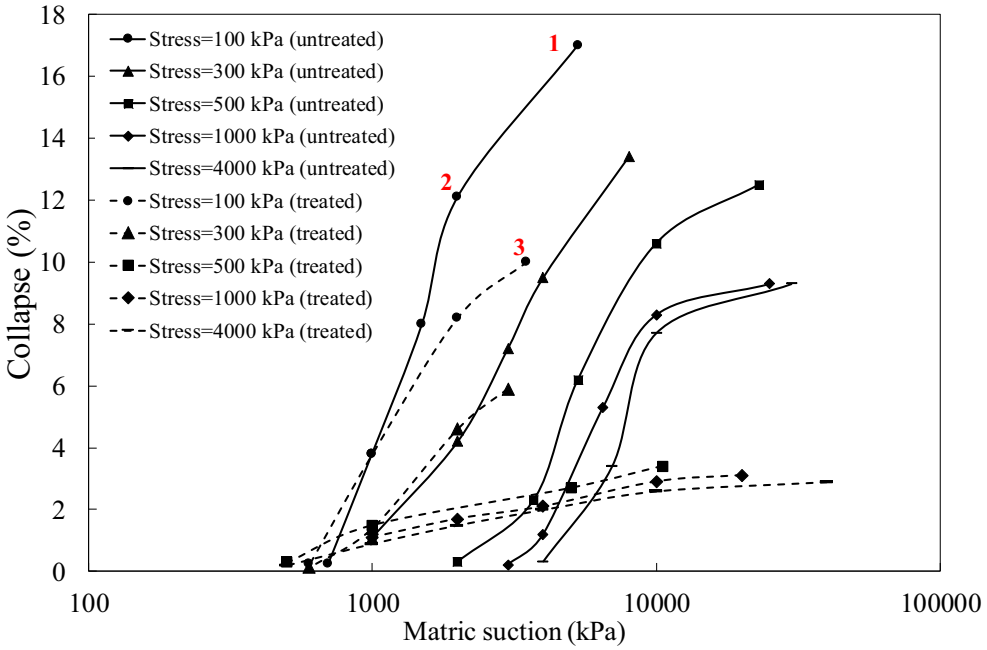

Fig. 10. Influence of suction change on collapse value.

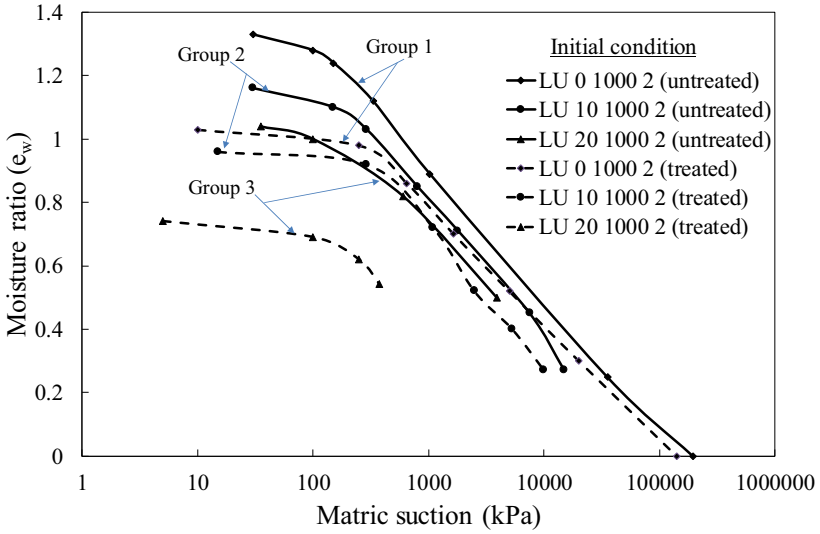

Fig. 11. SWCC below the virgin compression at operational stress = 2 kPa.

As the slopes of the transition zone, presented in Fig. 5, approached together after a suction value of 40,00 kPa for the untreated soil, it can be noticed in Fig. 8 that the void ratio–moisture ratio relationship followed the quadratic polynomial function [Eq. (1)] for suctions higher than 4,000 kPa. However, it followed the cubic polynomial function [Eq. (2)] for suction below 4,000 kPa.

$$e = ae_w^2 + be_w + c \tag{1}$$

$$e = ae_w^3 + be_w^2 + ce_w + d \tag{2}$$

However, for lime-treated soil (Fig. 9), the relationship between void ratio and moisture ratio for each suction contour was found to be more complex as the slopes of transition zone approached together after reaching a high suction (approximately after suction of 10,000 kPa in Fig. 6). Fig. 9 reveals that this relation followed cubic polynomial function [Eq. (2)] for suction contours higher than 10,000 kPa, while it followed quartic polynomial [Eq. (3)] function for suction contours below 10,000 kPa.

$$e = ae_w^4 + be_w^3 + ce_w^2 + de_w + f \tag{3}$$

where a, b, c, d, and f = fitting parameters.

Collapse Measurement

To interpret the influence of suction on the collapse behavior, five sets of 1-D tests were conducted based on compaction stress values of 100, 300, 500, 1000, and 4,000 kPa. Fig. 10 presents the collapse potential for specimens compacted to different compaction and matric suction values (initial moisture content) and then wetted to the saturation.

To investigate the relationship between suction and volumetric behavior, two identical specimens were prepared at a certain moisture content and compacted statically to a certain compaction stress. For example, two identical untreated specimens were prepared at a moisture content of 21% (e_w = 0.57) and then compacted to the

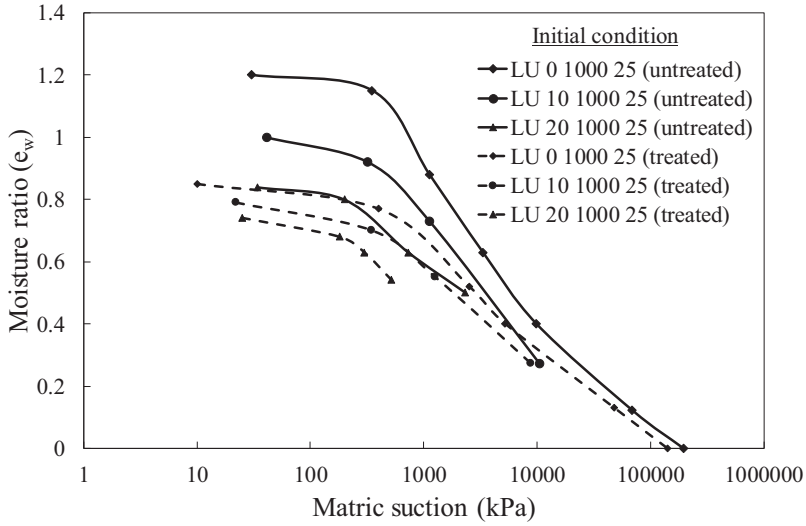

Fig. 12. SWCC below the virgin compression surface at operational stress = 25 kPa.

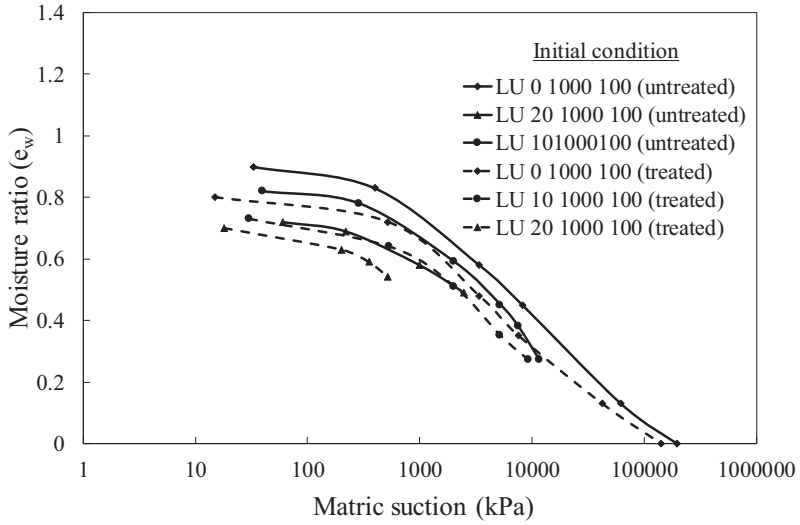

Fig. 13. SWCC below the virgin compression surface at operational stress = 100 kPa.

compaction stress of 100 kPa. The first specimen was used to measure suction, and it was found to be 5,300 kPa (Point 1 in Fig. 10). The other specimen was saturated under the same compaction stress. After saturation, the specimen volume reduced (i.e., collapsed), and volume changes were recorded until they became negligible. The collapse value was then calculated, and it was found to be 17% (Point 1).

The other two untreated specimens were prepared at a moisture content of 26% (e_w = 0.704) and then compacted to 100 kPa. The first specimen was used to measure suction, and it was found to be 2,000 kPa (Point 2). The other specimen was saturated under the same compaction stress, and the collapse value was found to be 12.1% (Point 2). The same procedure was followed for the specimens prepared at different moisture contents and then compacted statically to 100 kPa. Similarly for the specimens prepared at different moisture contents and then compacted statically to the compaction of 300; 500; 1,000; and 4,000 kPa.

For treated specimens, the same process was followed for the untreated specimens except that the specimens were cured for 7 days, and suction and collapse values were then obtained (Point 3). The same approach was repeated to generate other curves.

Suction Distribution below the Virgin Compression Surface

Fig. 11 presents three groups of specimens that were prepared based on initial moisture ratio. The first group included at least six identical dry specimens (moisture content of zero; $e_w = 0$) compacted statically to 1,000 kPa and then unloaded to the operational stress of 2 kPa. The treated specimens were cured for 7 days. Each specimen was wetted with different amounts of water (S_r from 0 to 100%) at the operational stress of 2 kPa. After wetting, the volume changes were recorded, and suction values were measured when the volume change became negligible. The SWCCs for the first group of untreated and treated clay specimens are given in Fig. 11 (LU 0 1000 2). The same procedure was repeated to obtain the SWCC for the second and third groups with the change that the specimens were prepared at moisture contents of 10 (e_w = 0.271) and 20% (e_w = 0.542) for the second and third groups, respectively. After unloading, the specimens were wetted from moisture content equivalent to 10% for Group 2 and 20% for Group 3 to full saturation, as given in Fig. 11 (LU 10 1000 2 and LU 20 1000 2). To cover a wide range of the SWCC below the surface, specimens were compacted under different initial moisture ratios to the compaction stress of 1,000 kPa and then unloaded to different operational stresses such as 25 kPa and 100 kPa, as presented in Figs. 12 and 13.

For specimens prepared at 0% moisture ratio, compacted to 1,000 kPa, and subsequently wetted with different amounts of water under the operational stresses of 2, 25, and 100 kPa, the specimen volume changes were measured after water was added. The void ratios were then calculated, and consequently, the relationship between void ratio and suction at a certain operational stress was obtained, as given in Fig. 14. By identifying the moisture ratio, void ratio, and suction for each specimen, the suction contours in e-e_w and e-e_w-log (σ) spaces at operational stresses of 2 kPa, 25 kPa, and 100 kPa are presented (Figs. 15, 16, and 17).

From Figs. 15, 16, and 17, it was obvious that for high-suction contours, the e-e_w relation followed the exponential function path [Eq. (4)]. However, as soon as the suction contours approached to the NCL, where S_r is equal to 100%, the e-e_w relation followed the quadratic polynomial function (Eq. (1).

$$e = e_0 + ae^{\left(\frac{e_w - e_{w0}}{b}\right)} \tag{4}$$

where e_0 and e_{w0} = initial void ratio and moisture ratio, respectively; and a and b = fitting parameters.

Swelling Measurements

The same procedure used to measure collapse was followed to prepare specimens and investigate the effect of suction on swelling behavior. The only exception was that the specimens were unloaded to a stress level less than the compaction stress and then wetted to reach the saturation.

Fig. 18 presents the results of three sets of 1-D tests based on operational stresses of 2, 25, and 100 kPa. The first set included three groups based on moisture contents (0, 10, and 20%) (e_w = 0, 0.271, and 0.542). The first group included preparing two identical specimens for the untreated and another two for the treated soils at zero moisture content (Points 1 and 4). The specimens were

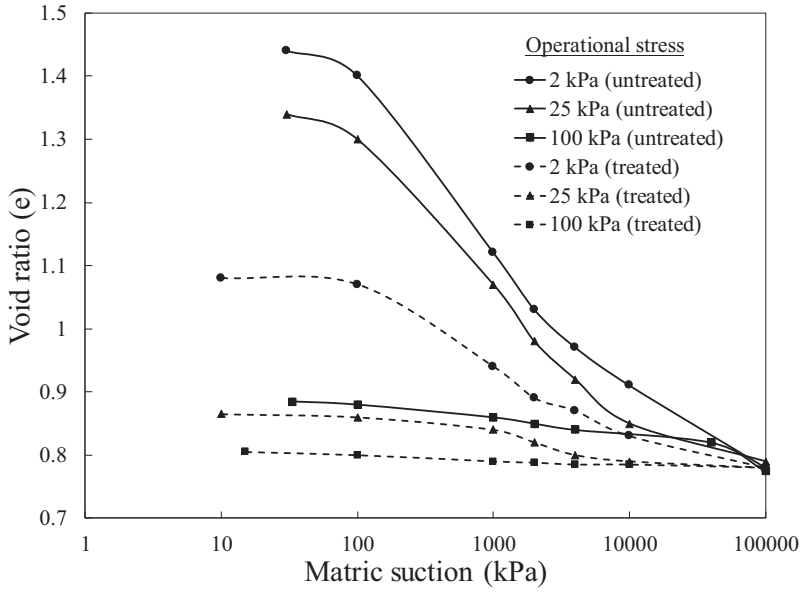

Fig. 14. Void ratio versus suction relation (below the virgin compression surface).

Int. J. Geomech., 2019, 19(2): 04018192

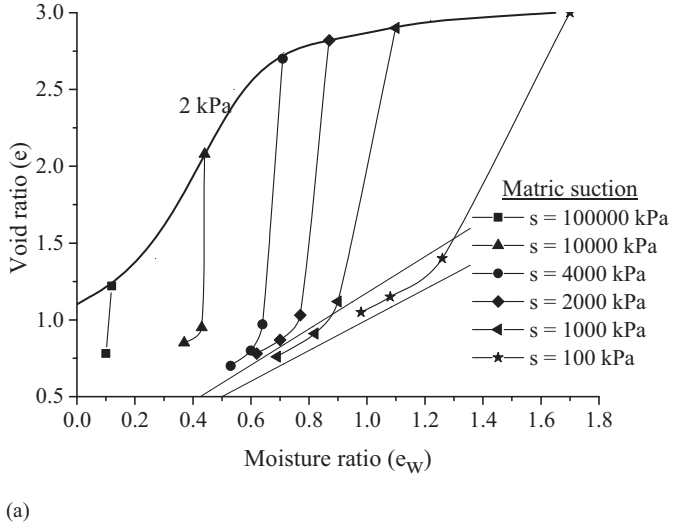

(a)

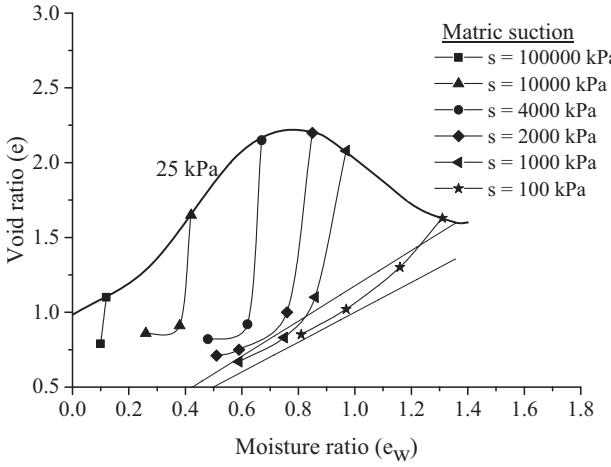

(b)

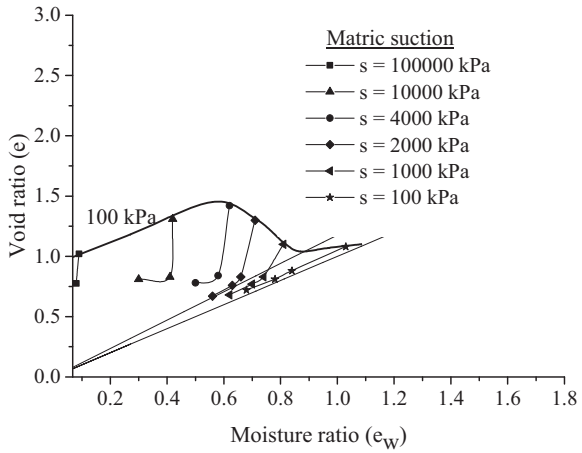

(c)

Fig. 15. Suction contours below the surface for untreated clay: (a) 2 kPa; (b) 25 kPa; and (c) 100 kPa.

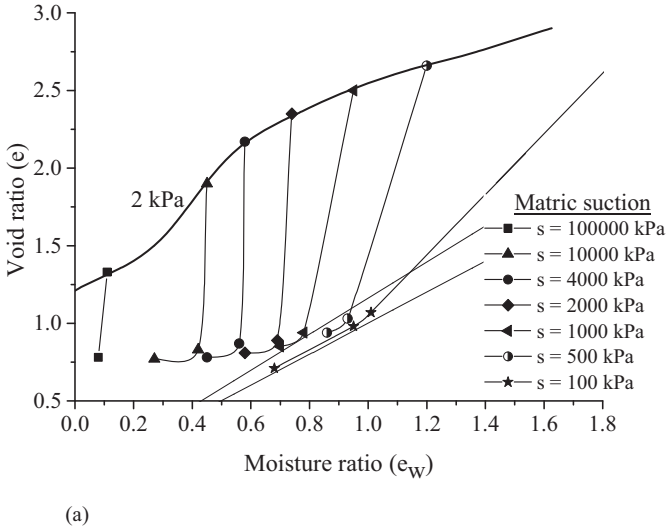

(a)

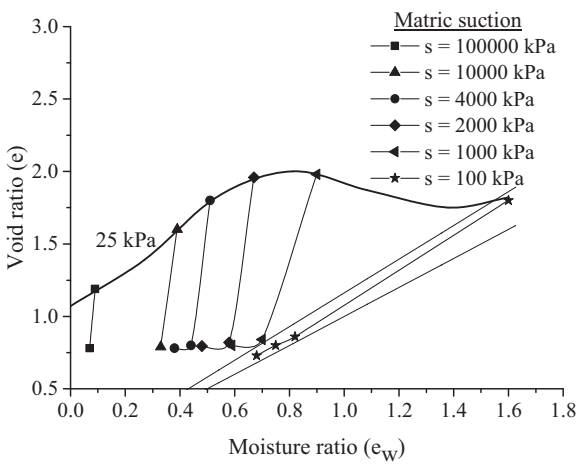

(b)

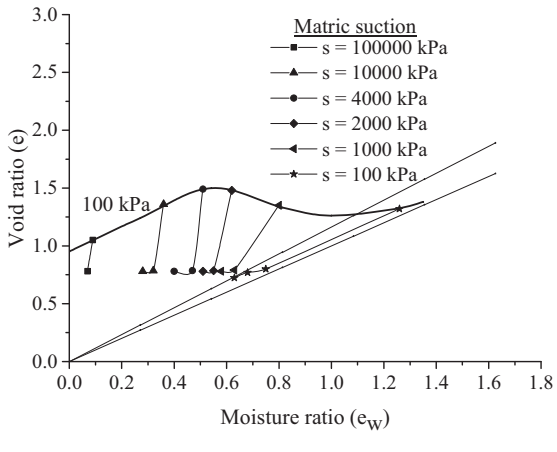

(c)

Fig. 16. Suction contours below the surface for lime-treated clay: (a) 2 kPa; (b) 25 kPa; and (c) 100 kPa.

compressed statically to 1,000 kPa and then unloaded to 2 kPa. The treated specimens were cured for 7 days. One specimen was used to measure the suction, and the values were found to be 190,000 kPa and 140,000 kPa for the untreated and lime treated specimens, respectively (Points 1 and 4), while the other specimen was then saturated. After saturation, the volume of specimen increased, and the increase in volume change (i.e., swell) was recorded. Once this change became negligible, the test was stopped, and the final swelling value was obtained. The final swelling value was found to be 30.1% for the untreated specimen and 14.8% for the lime-treated specimen (Points 1 and 4 in Fig. 18).

Int. J. Geomech., 2019, 19(2): 04018192

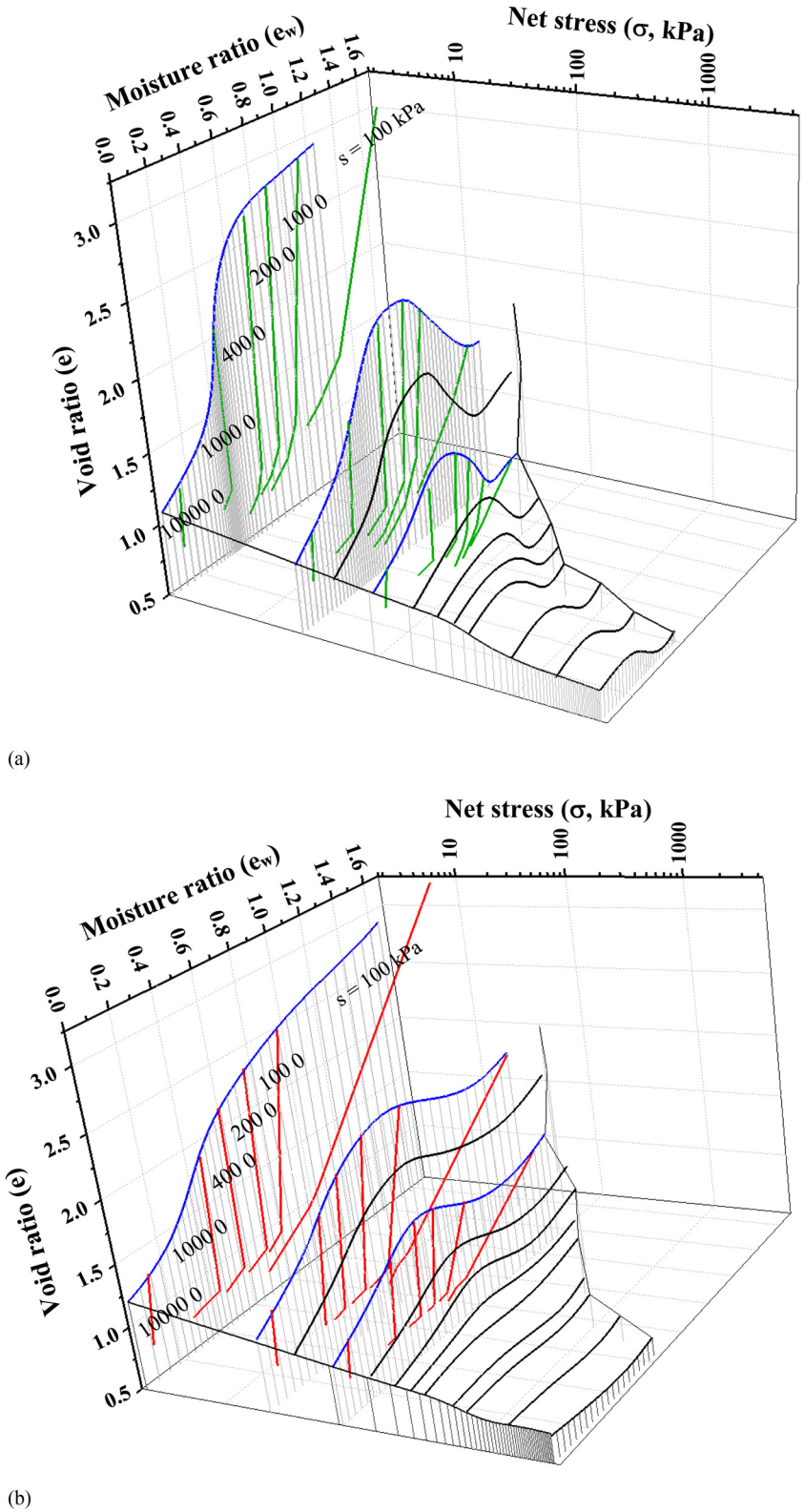

Fig. 17. Suction contours below the surface: (a) untreated clay; and (b) lime-treated clay.

The same procedure was followed for the second and third groups with the change that the specimens were prepared at moisture contents of 10%, e_w = 0.271, (Points 2 and 5); and 20%, e_w = 0.542, (Points 3 and 6), respectively. The same steps were repeated for the second and the third sets of tests except that the operational stress was changed to 25 kPa and 100 kPa, respectively.

Discussion

From Figs. 5 and 6, it was evident that as the net stress increased, the SWCC moved downward. Fig. 5 (for the untreated soil) revealed that the range of boundary effect zone increased as compaction stress increased with this zone extended from suction value of 300 kPa (for

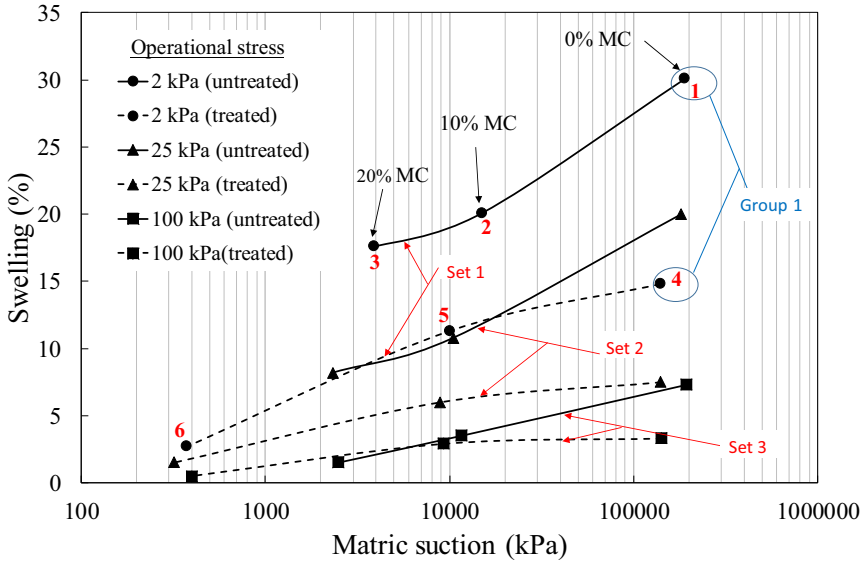

Fig. 18. Influence of suction change on swelling.

compaction stress of 100 kPa) to suction value of 3,000 kPa (for compaction stress of 4,000 kPa). This means that as the compaction stress increases, the void ratio decreases, and consequently, higher suction is required to cause air to enter the pores of soil. However, Fig. 6 (for the treated soil) revealed that the average range of boundary effect zone extended to the suction value of 80 kPa. This value, if compared with the untreated soil, indicated that the suction required to cause air to enter the pores of soil was dropped after treatment. The reason for this is lime contributes to reduce collapse value. The reduction in void ratio after stabilization will be less than that of the untreated soil (void ratio after stabilization will be higher than of untreated soil). Consequently, the suction force required to cause air to enter the pores of the treated soil is less than of the untreated soil. At a certain stress, the treated soil needed more moisture content to reach full saturation compared to the untreated soil. The reason for this behavior can be explained by the fact that the cation exchange process for lime-treated clay demands water to progress.

By focusing on the relationship between void ratio and suction for both soils (Fig. 7), it was obvious that the void ratio increased as suction increased. Furthermore, the change in void ratio decreased as net stresses increased. The change in void ratio values for the untreated soil was higher than the treated soil, and that is evidence of improvement.

Fig. 10 gives the influence of suction on the volumetric behavior, indicating that all specimens collapsed after wetting and the collapse values increased as the specimen suction (directly after compaction) increased. Furthermore, the collapse values increased as compaction stress decreased. Although the expansive clay was treated with lime at OLC, the treated clay was considered to be categorized as high collapsible (ASTM 2003; Rafie et al. 2008) when it was prepared at a suction higher than 2,000 kPa and wetted under a compaction stress less than 300 kPa.

Figs. 11, 12, and 13 represent the SWCCs below the surface. It was evident that the first part of the SWCC of the untreated specimen started with a moisture ratio higher than of the treated specimen. The reason for this behavior was that the behavior of soil below the surface described the swelling path after adding water. This path either remained below the surface after reaching the saturation or reached the surface, and that depended on the gradient of this path (Al-Taie et al. 2016). The swelling path gradient of the untreated soil was higher than of the treated soil. Therefore, it was expected that the untreated specimen reached the saturation condition with a moisture content higher than that of the lime-treated specimen, and consequently, the air entry value for untreated specimen was less than for the treated specimen.

Fig. 18 revealed that the specimens swelled after adding water, and these values increased as the suction of the specimens (directly after unloading) increased at a constant operational stress. Furthermore, the swelling values decreased as the operational stress increased. It is also important to mention that Fig. 18 found a significant swelling occurred when the treated specimen prepared at suction ≥ 10,000 kPa (moisture content ≤ 10%), then compacted to 1,000 kPa, and then wetted under operational stresses ≤ 25 kPa. To check these results, two identical specimens were prepared at a suction of 10,000 kPa (10% moisture content) and then loaded to 1,000 kPa. One specimen unloaded to 25 kPa and then wetted to the saturation. The swelling value was then obtained. The other specimen was cured for 7 days, and then the same procedure was followed to obtain the swelling value. It was noticed that the difference in swelling values was small and can be neglected. This behavior can be attributed to the mechanism of reaction between lime and clay. The first reaction began after adding water to the clay–lime mixture. The hydrated lime dissociated to Ca^{+2} and $2(OH)^{-1}$ ions, and consequently, the cation exchange, flocculation, and agglomeration started. That means enough water should be provided to start the stabilization process. As a result, adding a small amount of water to the clay would not affect the stabilization process during curing. However, the OLC was obtained at OMC, and thus, there was enough water to start the stabilization process during curing.

Conclusions

A series of laboratory tests was performed to investigate the influence of lime stabilization of an expansive clay soil based on volumetric behavior and the SWCC. The soil specimens were treated with lime at OLC (specimens were prepared at OMC and MDD and subjected to pressure of 25 kPa), and then virgin compression surface was established for both clays. The SWCCs were obtained at and below the surface under different stress levels. The collapse and swelling potential were tested under a wide range of moisture ratios and stress levels. This study concluded that although the soil

specimens were treated with lime at the OLC, the treated specimens were considered to be categorized as highly collapsible when the specimens were prepared at a suction higher than 2,000 kPa and wetted under a compaction stress less than 300 kPa. Furthermore, a significant swelling occurred when the treated specimen prepared at suction ≥ 10,000 kPa (moisture content ≤ 10%), compacted to 1,000 kPa, and then wetted under operational stresses ≤ 25 kPa.

Acknowledgments

The first author acknowledges the Republic of Iraq, Ministry of Higher Education and Scientific Research for the postgraduate research award. The last author is grateful to the financial support from the Thailand Research Fund under the TRF Senior Research Scholar Program Grant RTA5980005.

References

Al-Taie, A., M. M. Disfani, R. Evans, A. Arulrajah, and S. Horpibulsuk. 2016. "Swell-shrink cycles of lime stabilized expansive subgrade." *Procedia Eng.* 143: 615–622. https://doi.org/10.1016/j.proeng.2016.06.083.

Al-Taie, A., M. M. Disfani, R. Evans, A. Arulrajah, and S. Horpibulsuk. 2018. "Impact of curing on behaviour of basaltic expansive clay." *Road Mater. Pavement Des.* 19 (3): 624–645. https://doi.org/10.1080/14680629.2016.1267660.

AS (Standards Association of Australia). 2008. *Methods of testing of testing soils for engineering purposes—Soil classification tests—Determination of the linear shrinkage of a soil-standard method.* AS1289.3.4.1. Sydney, Australia: AS.

ASTM. 1994. *Standard test method for measurement of soil potential (suction) using filter paper*. D5298. West Conshohocken, PA: ASTM.

ASTM. 2000a. *Standard test method for liquid limit, plastic limit, and plasticity index of soils*. D4318. West Conshohocken, PA: ASTM.

ASTM. 2000b. *Standard test methods for laboratory compaction characteristics of soil using standard effort (12,400 ft-lbf/ft3)*. D698. West Conshohocken, PA: ASTM.

ASTM. 2003. *Standard test method for measurement of collapse potential of soils*. D5333. West Conshohocken, PA: ASTM.

ASTM. 2007. *Standard test method for particle size analysis of soils*. D422. West Conshohocken, PA: ASTM.

ASTM. 2010. *Standard test methods for specific gravity of soil solids by water pycnometer*. D854. West Conshohocken, PA: ASTM.

ASTM. 2011. *Standard practice for classification of soils for engineering purposes (unified soil classification system)*. D2487. West Conshohocken, PA: ASTM.

ASTM. 2016. *Standard test methods for determination of the soil water characteristic curve for desorption using hanging column, pressure extractor, chilled mirror hygrometer, or centrifuge*. D6836. West Conshohocken, PA: ASTM.

Bryson, L. S., I. C. Gomez-Gutierrez, and T. C. Hopkins. 2011. "Correlations between geotechnical properties and the swell behavior of compacted shales." in *Geo-Frontiers Congress 2011: Advances in geotechnical engineering*, Geotechnical Special Publication 211, 4119–4128. Reston, VA: ASCE. https://doi.org/10.1061/41165(397)420.

Chinkulkijniwat, A., S. Horpibulsuk, S. Yubonchit, T. Rakkob, R. Goodary, and A. Arulrajah. 2015. "Laboratory approach for faster determination of the loading-collapse yield curve of compacted soils." *J. Mater. Civ. Eng.* 28 (3): 04015148. https://doi.org/10.1061/(ASCE)MT.1943-5533.0001432.

Ciancio, D., C. T. S. Beckett, and J. A. H. Carraro. 2014. "Optimum lime content identification for lime-stabilised rammed earth." *Constr. Build. Mater.* 53: 59–65. https://doi.org/10.1016/j.conbuildmat.2013.11.077.

Colmenares Montanez, J. E. 2002. "Suction and volume changes of compacted sand bentonite mixtures." Ph.D. thesis, Imperial College of Science, Technology and Medicine, Univ. of London. http://hdl.handle.net/10044/1/7775.

Dineen, K., J. E. Colmenares, A. M. Ridley, and J. B. Burland. 1999. "Suction and volume changes of a bentonite-enriched sand." *Proc. Inst. Civ. Eng. Geotech. Eng.* 137 (4): 197–201. https://doi.org/10.1680/gt.1999.370405.

Fredlund, D. G. 2000. "The 1999 R.M. Hardy lecture: The implementation of unsaturated soil mechanics into geotechnical engineering." *Can. Geotech. J.* 37 (5): 963–986. https://doi.org/10.1139/t00-026.

Fredlund, D. G. 2006. "Unsaturated soil mechanics in engineering practice." *J. Geotech. Geoenviron. Eng.* 132 (3): 286–321. https://doi.org/10.1061/(ASCE)1090-0241(2006)132:3(286).

Fredlund, D. G., and H. Q. Vu. 2003. "Numerical modelling of swelling and shrinking soils around slabs-on-ground." In *Proc., Post-Tensioning Institute Annual Technical Conf.* Huntington Beach, CA: Post-Tensioning Institute (PTI).

Fredlund, D. G., and A. Xing. 1994. "Equations for the soil-water characteristic curve." *Can. Geotech. J.* 31 (4): 521–532. https://doi.org/10.1139/t94-061.

Haeri, S. M., A. Khosravi, A. A. Garakani, and S. Ghazizadeh. 2016. "Effect of soil structure and disturbance on hydromechanical behavior of collapsible Loessial soils." *Int. J. Geomech.* 17 (1): 04016021. https://doi.org/10.1061/(ASCE)GM.1943-5622.0000656.

Iyer, K., S. Jayanth, S. Gurnani, and D. N. Singh. 2012. "Influence of initial water content and specimen thickness on the SWCC of fine-grained soils." *Int. J. Geomech.* 13 (6): 894–899. https://doi.org/10.1061/(ASCE)GM.1943-5622.0000265.

Jones, E. W., Y. H. Koh, B. J. Tiver, and M. A. Wong. 2009. "Modelling the behaviour of unsaturated, saline clay for geotechnical design." *School of Civil Environment and Mining Engineering*. Adelaide, Australia: Univ. of Adelaide.

Kodikara, J. 2012. "New framework for volumetric constitutive behaviour of compacted unsaturated soils." *Can. Geotech. J.* 49 (11): 1227–1243. https://doi.org/10.1139/t2012-084.

Krishnapillai, S. H., and N. Ravichandran. 2012. "New soil-water characteristic curve and its performance in the finite-element simulation of unsaturated soils." *Int. J. Geomech* 12 (3): 209–219. https://doi.org/10.1061/(ASCE)GM.1943-5622.0000132.

McAndrew, J., and M. A. H. Marsden. 1973. *Regional guide to Victorian geology*. Melbourne, Australia: School of Geology, Univ. of Melbourne.

Murray, E. J., and V. Sivakumar. 2010. *Unsaturated soils: A fundamental interpretation of soil behaviour*. London: John Wiley & Sons.

Pasha, A. Y., A. Khoshghalb, and N. Khalili. 2016. "Pitfalls in interpretation of gravimetric water content–based soil-water characteristic curve for deformable porous media." *Int. J. Geomech.* 16 (6): D4015004. https://doi.org/10.1061/(ASCE)GM.1943-5622.0000570.

Puppala, A. J., K. Punthutaecha, and S. K. Vanapalli. 2006. "Soil-Water Characteristic Curves of Stabilized Expansive Soils." *J. Geotech. Geoenviron. Eng.* 132 (6): 736–751. https://doi.org/10.1061/(ASCE)1090-0241(2006)132:6(736).

Rafie, B. M. A., R. Z. Moayed, and M. Esmaeli. 2008. "Evaluation of soil collapsibility potential: A case study of Semnan railway station." *Electron. J. Geotech. Eng.* 13: 1–7.

Richards, B., P. Peter, and R. Martin. 1984. "The determination of volume change properties in expansive soils." In *Fifth Int. Conf. on Expansive Soils 1984: Preprints of papers*, 179. Adelaide, Australia: Institution of Engineers.

Romero Morales, E. 1999. "Characterisation and thermo-hydro-mechanical behaviour of unsaturated Boom clay: An experimental study." Ph.D. thesis, Departament d'Enginyeria del Terreny, Cartogràfica i Geofísica, Universitat Polite'cnica de Catalunya.

UMS. 2013. "HYPROP-Laboratory evaporation method for the determination of pF-curves and unsaturated conductivity." Accessed August 29, 2013. http://www.ums-muc.de/en/products/soil_laboratory/hyprop.html.

Van Der Merwe, D. H. 1964. "The prediction of heave from the plasticity index and percentage clay fraction." *South Afr. Inst. Civ. Eng.* (6): 103–107.

Zhao, H., L. Ge, T. M. Petry, and Y.-Z. Sun. 2014. "Effects of chemical stabilizers on an expansive clay." *KSCE J. Civ. Eng.* 18 (4): 1009–1017. https://doi.org/10.1007/s12205-013-1014-5.